



**UNIVERSITY OF
LIMERICK**
OLLSCOIL LUIMNIGH

**Bernal
Institute**



Stokes
Microfluidics

**MODULAR MICROPUMP FLUIDIC SYSTEMS: FOR
SYSTEM REQUIRING ULTRA-RELIABILITY, HIGH
PERFORMANCE, AND A COMPACT DESIGN**

ESA CONTRACT No. 4000134596/21/NL/GLC/ov

Executive Summary Report

Dr Valeria Nico & Dr Eric Dalton

Stokes Laboratories, Bernal Institute, University of Limerick

Executive Summary Report

INTRODUCTION

Due to the ongoing miniaturization and increased performance of electronics devices alternative cooling methods are required, specifically mechanical pumping loops (MPL). Passive two-phase loop is not capable of cooling the ESA expected power densities up to 300 W/m², pumped two-phase loops are forecasted to replace their passive counterparts. According to Lapensée et. al., "the most important component of a MPL is the pump and a pump failure directly results in MPL system failure, a reliable pump is therefore of vital importance". Wits et. al. noted that in addition to a reliability of >20 years, the micro-pump is required to withstand a working pressure of 60 bar, and to achieve a minimum flow rate of 5 ml/min.

The University of Limerick (UL) team has developed an ultra-reliable magnetic shuttle pump (MSP) features a two counter-wound solenoid coils, which are used to oscillate a neodymium shuttle magnet. As part of the project, a manifold of five pumps in parallel and a flowmeter were integrated into a flow control unit that can withstand high working pressures (> 60 bar) and the harsh vibrations involved in space applications. Such flow control unit was finally used in a two-phase MPL demonstrator to show the feasibility of the integration.

1 Flow control unit technology

In order to control the flow rate in the demonstrator, a flow control unit consisting of a manifold of five pumps and a flow sensor was developed. A controller board with dedicated user interface was also realised to power the manifold and read the flow sensor.

Five pumps developed by UL were connected in parallel in a flat arrangement manifold. Information regarding the working principle of the pump can be found in Nico, V. and Dalton, E., 2021. *Modelling and Experimental Characterisation of a Magnetic Shuttle Pump for Microfluidic Applications. Sensors and Actuators A: Physical*, p.112910. The flat arrangement was preferred for better integrations with racks used in CubeSats and its design is illustrated in Figure 1 and Figure 2. The manifold consists of two stainless steel plates (Figure 1a) with an G1/8 threaded inlet (or outlet) and five M4 threaded holes for the pumps. Pump connectors have also threads to prevent leakages associated with the use of the O-rings. Right hand threads are used on the inlet plate and inlet connectors of the pump, while left hand threads are used on the outlet plate and on the outlet connectors of the pumps as shown in Figure 1b. A photo of the assembled manifold is shown in Figure 2.

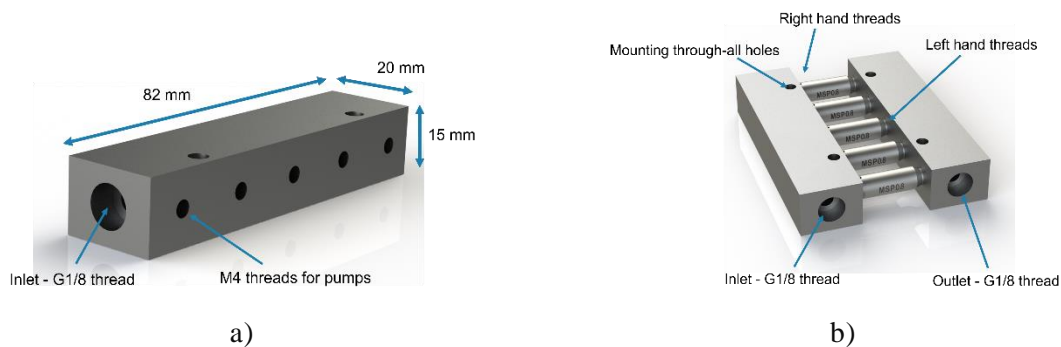


Figure 1 – Manifold design: a) plate; b) 3D view of the manifold



Figure 2 – Photo of the assembled manifold

Due to the high-pressure requirements, a purpose-built flow sensor designed by UL was selected for integration in the flow control unit. A schematic of the flowmeter is reported in Figure 3. flowmeter features a ferrite core that moves inside a corrosion-resistant tube. A small hole is present in the ferromagnetic core to allow the fluid to flow. By varying the size of the hole, it is possible to change the range of the flow rates that the device can measure.

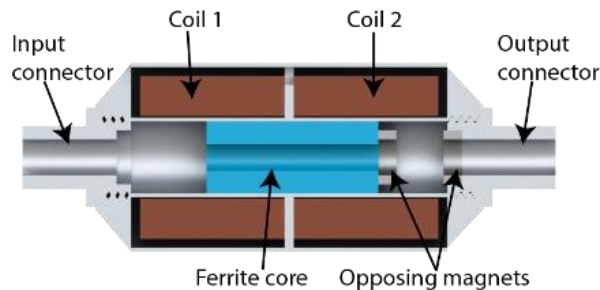


Figure 3 - Schematics of the flowmeter

The controller board is based on Adafruit M4 express feather board. Five independent 3 W D type audio power amplifier were used to power independently the pumps as shown in Figure 4a. A transistor and a regulated 3.3 V source were employed for powering the flowmeter (Figure 4b) while a diode, capacitor and resistor allows the AC signal from the sensor to be converted to an DC signal to be read.

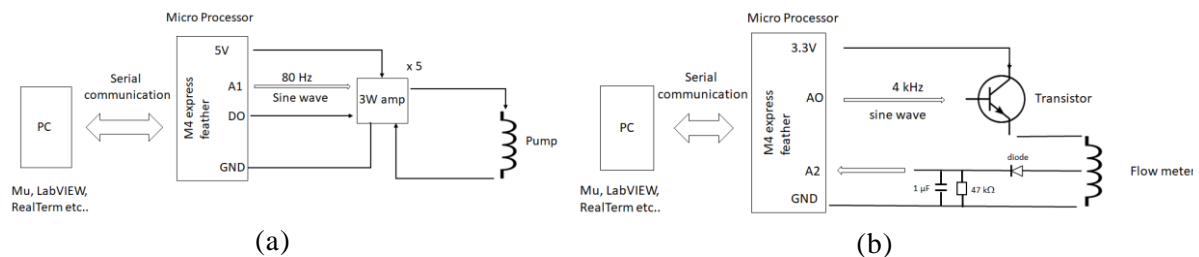


Figure 4 -Schematic of the flow control unit: (a) pumps driver; (b) flow sensor control

2 Manifold experimental characterisation

A range of tests were carried out to fully characterise the manifold and to verify it met the high working pressure requirements. In particular, the electromagnetic field and the microvibrations generated by the manifold were measured to verify that UL's technology met ESA's requirements, while pressure tests were carried out to verify that the manifold could withstand pressures up to 150 bar. Vibration tests were also carried out at an external facility to verify the capability of the manifold to withstand the harsh acceleration environment associated with take-off and landing. Finally, corrosion testing in liquid ammonia was carried out.

In order to measure the electromagnetic field, the manifold was powered with 1 W per pump and the AC/DC magnetic field and the electric field were measured as function of distance from the manifold.

For distances greater than 10 mm, the amplitude of both the AC and DC magnetic field was lower than 1.2 mT, while the amplitude of the electric field was lower than 2.6 V/m.

The measurement of the microvibrations generated by the manifold was carried out at in the ESTEC Test Centre using a Kistler 9255A dynamometer. The manifold was filled with Novec 7100 and the inlet and outlet were connected so that the manifold was pumping fluid in a closed loop to simulate normal working conditions as shown in Figure 9.

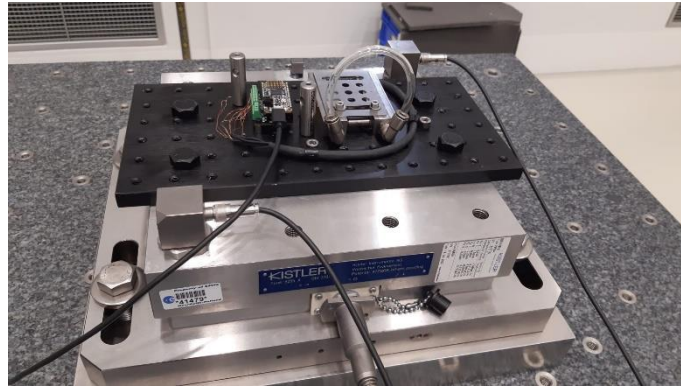


Figure 5 - Setup used for testing the microvibrations generated by the manifold.

Since the internal shuttle magnets in the pumps could oscillate in phase or in anti-phase depending on how pumps were electrically connected to the control board, four pumps only were powered, and different wiring configurations were considered to determine if vibrations could be reduced by allowing the shuttle magnets to oscillate in anti-phase. Several input pump power values were considered and Figure 9 shows the trend of the rms of the force X component as function of different pump powers.

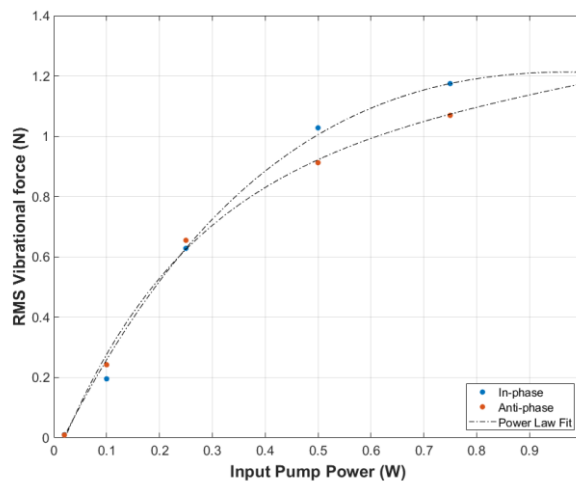


Figure 6 - RMS of the force X-components as function of power per pump for in-phase and anti-phase configurations.

As reported in the next section, the manifold was integrated into a two-phase MPL and it will be shown that depending on the input pump power, different payloads can be dissipated. The data presented in the next section were combined with the microvibration data to evaluate the amount of vibrations generated as function of cooling capacity and results are shown in Figure 7. When Novec 7100 is used as working fluid, it is possible for a 5 W/cm² thermal flux to be cooled with a vibration level of 14 mN if pumps are connected in anti-phase oscillation. A maximum thermal flux of 23.8 W/cm² could instead be cooled with a vibration level of 0.9 N.

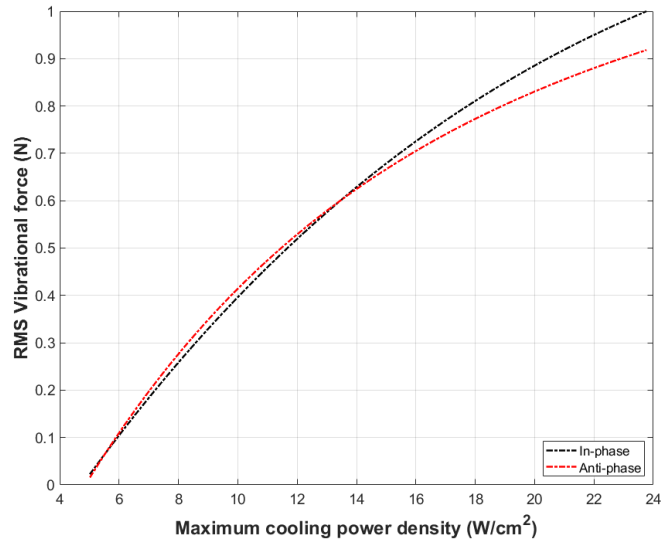


Figure 7 - RMS of the force X-component as function of maximum cooling power density for in-phase and anti-phase oscillations

Vibration tests were carried out externally on the manifold and on the electronic board to verify if they could withstand the harsh acceleration environment of take-off and landing. The vibration profiles and testing procedure used were the one reported on ECSS-E-ST-10-03A. To verify that the manifold was not damaged, the pressure-flow rate characterisation curve was carried out before and after the vibration test. The curve is reported in Figure 9. As visible from the curve, the manifold was not damaged by the test.

After the vibration test, the same manifold was pressurised up to 150 bar to verify that sealings were not damaged. To avoid potential damages to the pump valves due to pressure imbalances during the pressurisation, the manifold was tested in a loop as illustrated in Figure 8. Pressure was held for 10 minutes, and no leakages were detected.

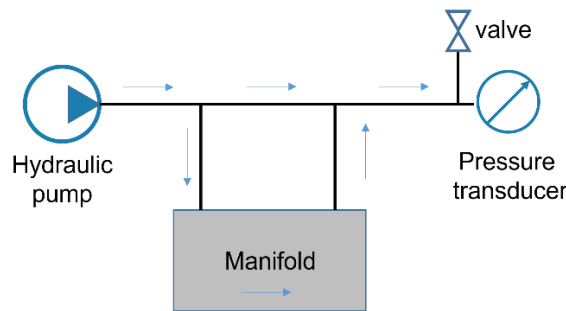


Figure 8 - Schematic of loop used to pressurise the manifold.

The manifold was characterised again after the pressurisation to verify that pumps were not damaged, and the characterisation curve is reported in Figure 9. The input power to each pump was 1W and the excitation frequency was 80 Hz. As visible, the manifold was not damage and the maximum pressure achieved after the pressure test was 47 kPa, while the maximum flowrate was 174 ml/min.

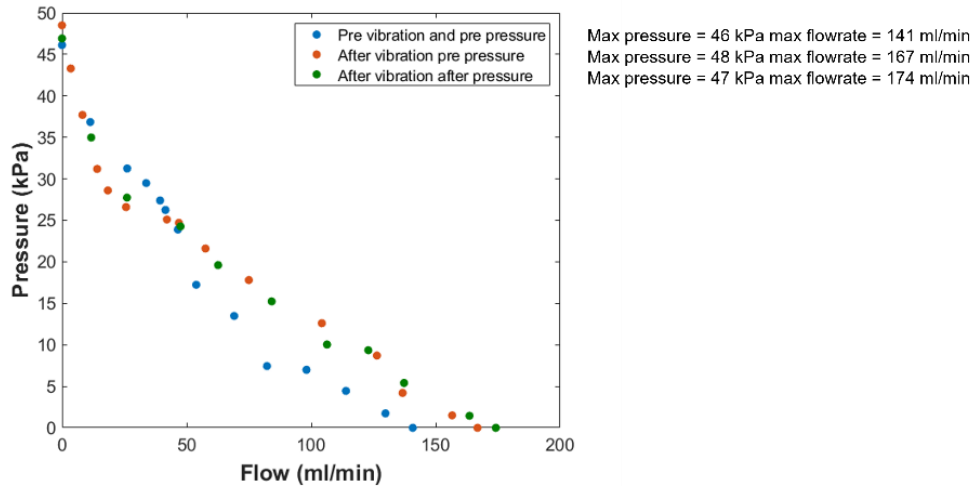


Figure 9 - Manifold characteristics at 1 W input power per pump before, after the vibration tests and after the pressurisation.

Finally, to verify that the pump's components were compatible with ammonia, a titanium pump body and a shuttle magnet coated in titanium nitride were placed in a vessel filled with 4.7 ml of liquid ammonia. The components were kept in the vessel for 117 days and once ammonia was released, samples were inspected and compared with new reference components to check if corrosion happened.

To verify that corrosion did not happen, imaging of the samples and of the references using an optical microscope were carried out and results are reported in Figure 10 and Figure. Figure 10 shows microscope images of the magnet after being in liquid ammonia (Figure 10a to Figure 10c) and of a new magnet (Figure 10d to Figure 10e) for different magnification levels. From the comparison of the images taken on the sample and on the reference, it is possible to note that corrosion is not present as surfaces look similar.

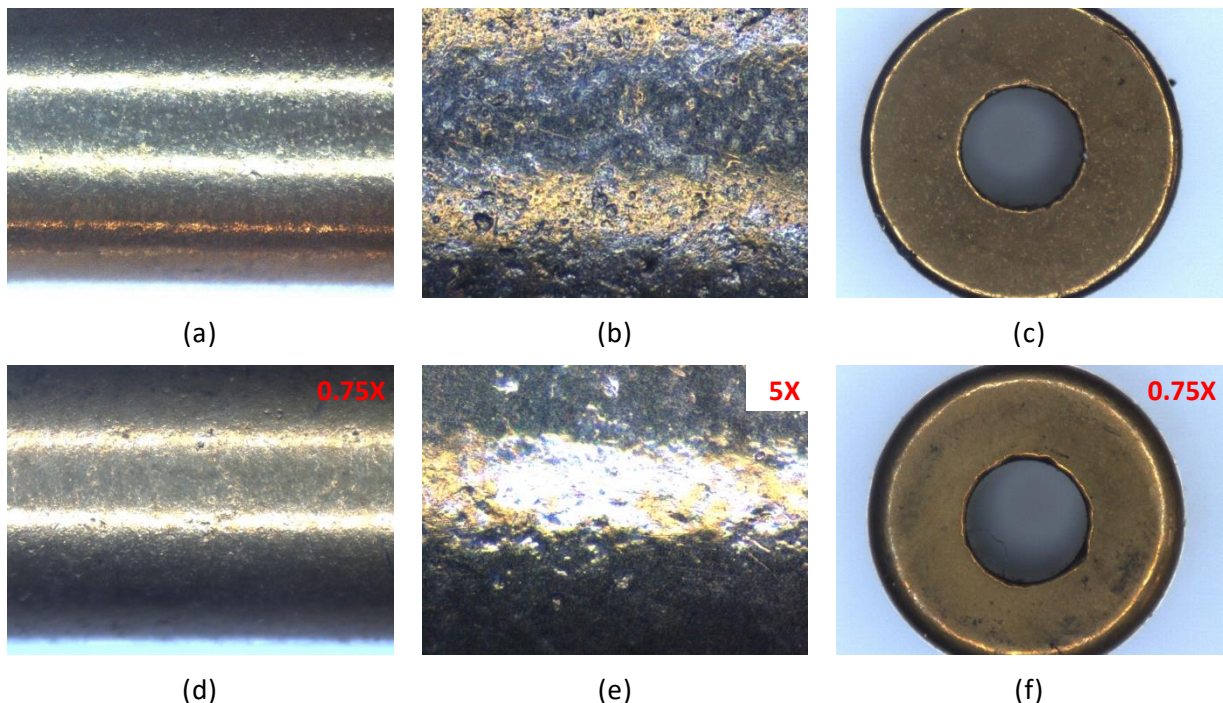


Figure 10 - Microscope images of magnets:(a)-(c) sample magnet that was placed in ammonia; (d)-(f) reference new magnet

Figure 11, instead, show microscope images of the pump body after being in liquid ammonia (Figure 11a and Figure 11b) and a new pump body (Figure 11c and Figure 11d) for different magnification levels. Also in this case, from the comparison of the images, it is possible to note that corrosion did not happen.

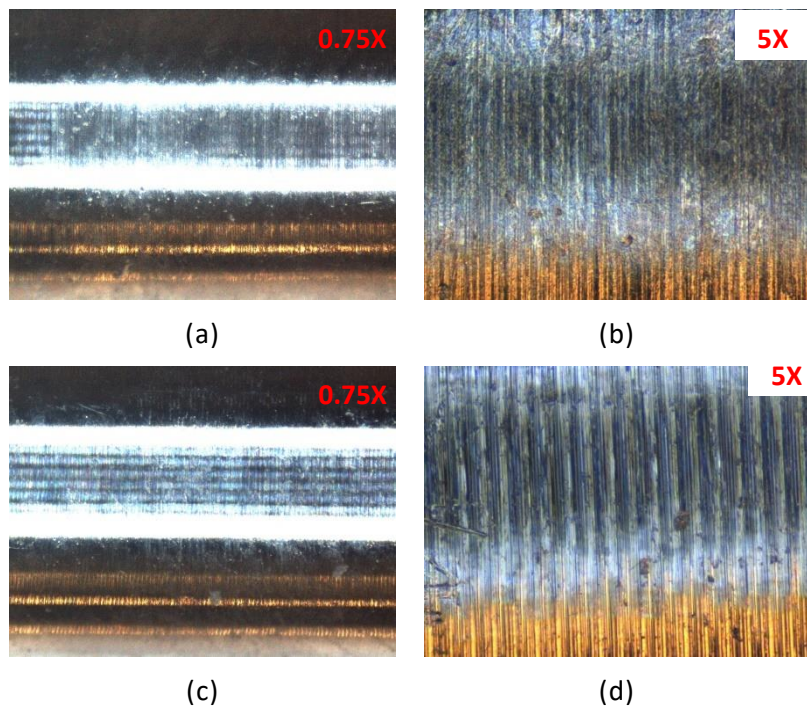


Figure 11 - Microscope images of the pump bodies: (a)-(b) sample pump body that was placed in ammonia; (c)-(d) reference new pump body.

3 Two-phase MPL demonstrator

The manifold and the flowmeter were integrated into a two-phase MPL demonstrator that uses Novec 7100 as working fluid. A schematic of the experimental setup is shown in Figure 12, while a photo is reported in Figure 13. Cartridge heaters in a copper block are used to simulate a payload, while an off-the-shelves Alphacool XPX 1U (total area 104 cm²) is used as evaporator to transfer heat from the heaters to the working fluid. A liquid-to-liquid NORDIC TEC Ba-12-30 heat exchanger is used as condenser to dissipate heat from the working fluid to an oil coolant. The temperature of the oil coolant bath can be set to simulate different condenser temperatures. Omega PXM409 pressure transducers are used to measure the pressure drop across the micropump, evaporator and condenser, while Type-K thermocouples are used to measure the temperature at various points in the cooling loop, as illustrated in Figure 12. Labview and NI data acquisition systems were used to monitor the system.

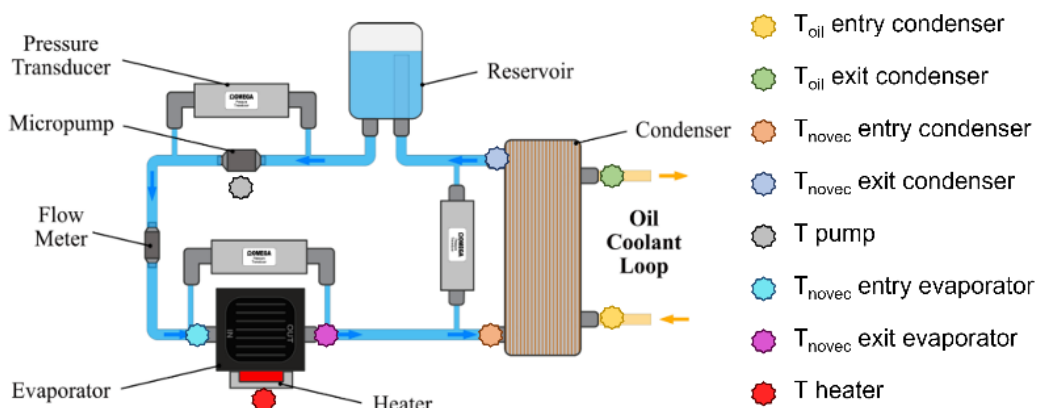


Figure 12 - Schematics of the two-phase MPL used. In the schematic a single micropump is represented instead of the manifold.

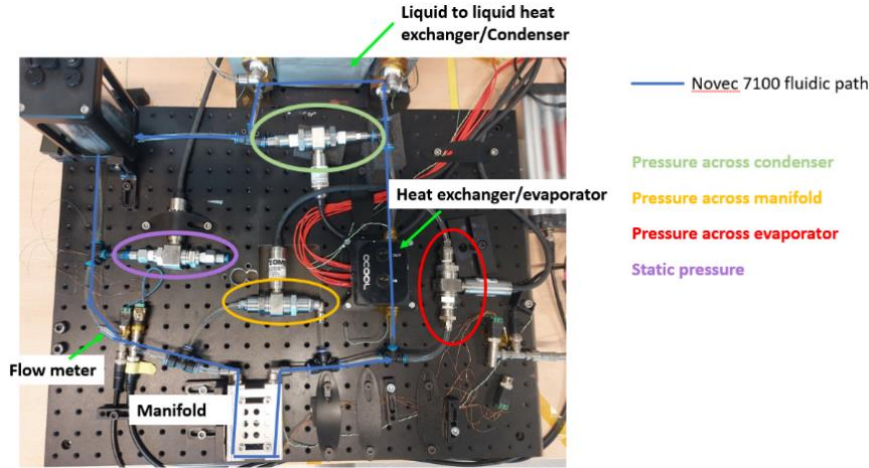


Figure 13 - Photo representing the MPL loop

Characterisation of the demonstrator was carried by powering the five pumps at different power levels but keeping the temperature of the secondary heat exchanger bath constant at 20°C. The heater power was varied from 0 W to 350 W (or until a heater temperature of 85°C was reached) and the heater temperature (T_{heater} in Figure 12) was recorded.

shows the trend of the temperature in the heater (T_{heater}) as function of heat absorbed (P_{heater}) by the Novec 7100 for five different manifold input power in the range 0.3 W to 1.5 W. The manifold input power was equally divided between each individual pump and it is given by the sum of each pump input power. By varying the manifold input power, the flow rate developed by the manifold varied from 52.68 g/min at 0.3 W to 123.81 g/min at 1.5 W.

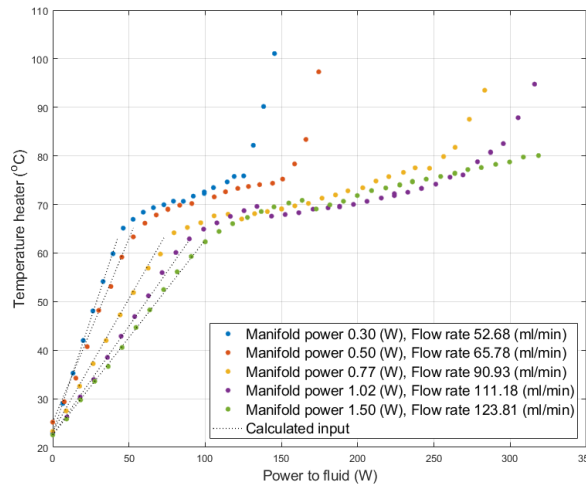


Figure 14 - Heater temperature increase as a function of heat absorbed by the fluid for five different manifold input power and thermal bath temperature of 20°C.

The power to the fluid (Q_{fluid}) was calculated in the sensible heat region from equation 1:

$$Q_{\text{fluid}} = c_p \dot{m}_{\text{novec}} (T_{\text{entry}}^{\text{evap}} - T_{\text{exit}}^{\text{evap}}) \quad (1)$$

where:

c_p is Novec 7100 heat capacity ($c_p = 1183 \text{ J/kg } ^\circ\text{C}$)

\dot{m}_{novec} is the mass flow rate of Novec 7100, calculated from $\dot{m}_{\text{novec}} = \dot{v}_{\text{novec}} \rho_{\text{novec}}$; \dot{v}_{novec} is the volume flow rate as measured and ρ_{novec} is 1.51 g/cm^3 .

$T_{\text{entry}}^{\text{evap}}$ and $T_{\text{exit}}^{\text{evap}}$ are the temperatures of the Novec 7100 at the entry and exit of the evaporator.

From Figure 14, it is possible to see that the trend for the five different manifold input powers is similar. Within a T_{heater} range of $\sim 25^{\circ}\text{C}$ to $\sim 66^{\circ}\text{C}$, there is an approximately linear relationship between P_{heater} and T_{heater} . In this range, the fluid is in the liquid state and absorbs sensible heat from the heater. Due to the variation of the mass flow rate of the fluid, there is a significant variation in power dissipated: from $P_{\text{heater}} = 46.2 \text{ W}$ at 0.3 W input power to $P_{\text{heater}} = 109 \text{ W}$ at 1.5 W input power. In the range $T_{\text{heater}} = 66^{\circ}\text{C}$ to $\sim 76^{\circ}\text{C}$, there is a small increase in temperature and phase change is observed in the working fluid. In this region latent heat is absorbed and evaporation occurs.

When evaporation is complete, the fluid becomes dry vapour and a sharp increase in T_{heater} is visible in Figure 14. This sharp increase is visible above $T_{\text{heater}} = \sim 76^{\circ}\text{C}$. The fluid cannot dissipate any more heat and the heater begins to overheat. The point at which the dry vapour region occurs is different for the five pump powers as it depends on the \dot{m}_{Novec} . It ranges from $P_{\text{heater}} = 125 \text{ W}$ at 0.3 W input power to $P_{\text{heater}} > 320 \text{ W}$ at 1.5 W input power. Due to the limitation of the cartridge heater used, it was not possible to test the manifold in the last configuration at higher values of P_{heater} .

4 Project outcomes

As part of the project, a manifold of five pumps in parallel and a flowmeter were integrated in a flow control unit that could withstand high working pressures.

Pressure tests up to 150 bar were carried out on the manifold and on the flowmeter to verify the capability of the devices to withstand high working pressures. The pressure was held for 10 minutes and neither deformations nor leaks were observed.

Environmental tests were carried out also on the manifold. For distances greater than 10 mm, the amplitude of both AC and DC magnetic field was lower than 1.2 mT, while the electric field amplitude was smaller than 2.6 V/m. The microvibrations generated by the manifold were also measured at ESTEC testing facility. By connecting pumps to allow anti-phase oscillations of the shuttle magnet, it was possible to reduce the generated microvibrations and it was estimated that when Novec 7100 is used as working fluid, it is possible for a 5 W/cm^2 thermal flux to be cooled with a vibration level of 14 mN if pumps are connected in anti-phase oscillation. A maximum thermal flux of 23.8 W/cm^2 could instead be cooled with a vibration level of 0.9 N.

Vibration tests were carried out on the manifold using the vibration profiles reported on ECSS-E-ST-10-03A. The vibration tests did not damage the manifold.

To identify corrosion, pump components were kept in a vessel 40% filled with liquid ammonia for 117 days. Once the vessel was open, components were inspected and compared with new ones. No corrosion or discoloration was detected.

Finally, a demonstrator was realised to evaluate the capability of the manifold to dissipate heat. Three tests were carried out considering different values of input power to the manifold; different numbers of working pumps; and different thermal bath temperature with three working pumps. The manifold could dissipate up to 320 W at 1.5W input electric power.